

The synthesis and properties of solution processable red-emitting phosphorescent dendrimers

Michael J. Frampton,^a Ebinazar B. Namdas,^b Shih-Chun Lo,^a Paul L. Burn*^a and Ifor D. W. Samuel*^b

^aChemistry Research Laboratory, Department of Chemistry, University of Oxford, Mansfield Rd, Oxford, UK OX1 3TA

^bOrganic Semiconductor Centre, School of Physics and Astronomy, University of St Andrews, North Haugh, St Andrews, Fife, UK KY16 9SS

Received 8th January 2004, Accepted 11th June 2004

First published as an Advance Article on the web 9th August 2004

We report methodology for the preparation of symmetric and asymmetric solution processable phosphorescent dendrimers that are comprised of 2-ethylhexyloxy surface groups, biphenyl based dendrons, and iridium(III) complex cores. The symmetric dendrimer has three dendritic 2-benzo[*b*]thiophene-2'-ylpyridyl (BTP) ligands with the dendritic ligands responsible for red emission. The asymmetric dendrimer has two dendritic 2-phenylpyridyl ligands and one unsubstituted BTP ligand. Iridium(III) complexes comprised of 2-phenylpyridyl ligands are normally associated with green emission whereas those containing BTP ligands emit red light. Red emission is observed from the asymmetric dendrimer demonstrating that emission occurs primarily from the metal-to-ligand charge transfer state associated with the ligand with the lowest HOMO–LUMO energy gap. The photoluminescence quantum yields (PLQYs) of the symmetric and asymmetric dendrimers were strongly dependent on the dendrimer structure. In solution the PLQYs of the asymmetric and symmetric dendrimers were $47 \pm 5\%$ and $29 \pm 3\%$ respectively. The photoluminescence lifetime of the emissive state of both dendrimers in solution was $7.3 \pm 0.1 \mu\text{s}$. In the solid state the comparative PLQYs were reversed with the symmetric dendrimer having a PLQY of $10 \pm 1\%$ and the asymmetric dendrimer a PLQY of $7 \pm 1\%$. The comparatively larger decrease in PLQY for the asymmetric dendrimer in the solid state is attributed to increased core–core interactions. The intermolecular interactions are greater in the asymmetric dendrimer because there is no dendron on the BTP ligand. Electrochemical analysis shows that charge is injected directly into the cores of the dendrimers.

Introduction

Full colour displays based on organic light-emitting diodes (OLEDs) require organic materials that emit red, green and blue light. For both fluorescent and phosphorescent materials, emitters with good colour co-ordinates have been produced. The advantage of phosphorescent emitters is that they can harvest both singlet and triplet excitons and hence lead to OLEDs with 100% internal quantum efficiencies. The main approach to phosphorescent OLEDs has been the development of small phosphorescent molecules that are processed by evaporation and of these the family of complexes based on iridium(III) have proved most successful.¹ For large area displays it is generally thought that solution processing will have an advantage over evaporation processing techniques. As a consequence there has been some effort in developing solution processed phosphorescent emitters.² One route investigated has been to blend a phosphorescent guest into a solution processable fluorescent host.³ An alternative approach to solution processable phosphorescent emitters is to use dendrimers that contain organometallic complexes. Although there have been a number of photophysical and electrochemical studies on dendrimers that contain metal complexes these have not been in the context of OLEDs.^{4,5} The dendrimers have generally contained non-conjugated dendrons with the measurements carried out in solution. More recently there has been work on dendrimers that contain conjugated dendrons and organometallic complexes.^{6,7} We have concentrated on developing dendrimers that contain rigid conjugated dendrons as solid state phosphorescent emitters that can be used as the emissive layer in OLEDs.⁷ Dendrimers have been prepared that

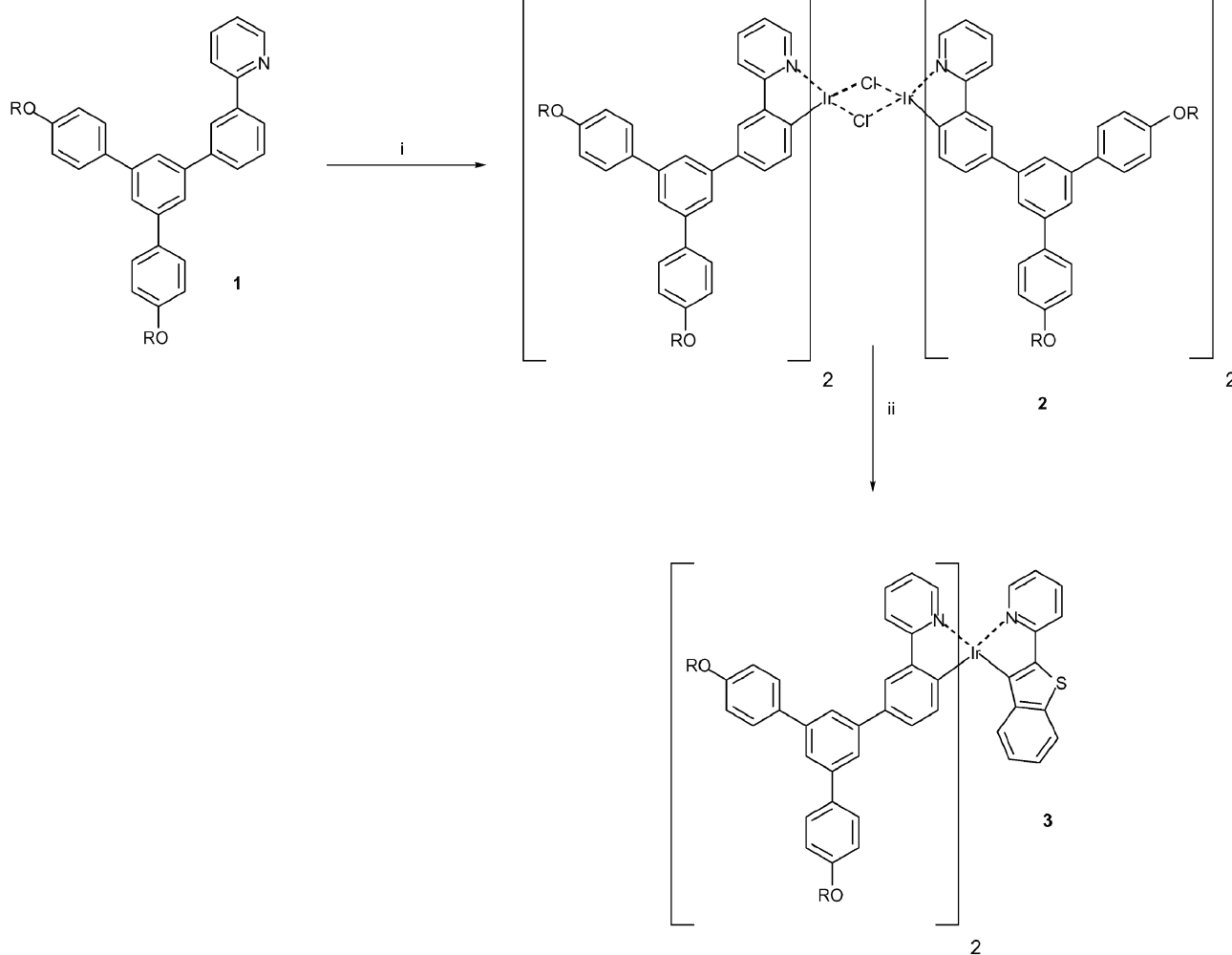
contain *fac*-tris(2-phenylpyridyl)iridium(III) cores, biphenyl based dendrons and 2-ethylhexyloxy surface groups. These materials have been used as the emissive layers in highly efficient OLEDs that emit green light.^{7b–e}

In pursuing materials for full colour displays we have now turned our attention to materials that emit red light. There have been a number of iridium(III) complexes that have been used in OLEDs to emit red.^{8–10} For this investigation we chose to develop dendrimers that contain cores based on iridium(III) complexes with one and three 2-benzo[*b*]thiophene-2'-ylpyridyl (BTP) ligands. Molecular BTP based iridium(III) complexes have been shown to have the required colour co-ordinates for full colour displays.^{1b} In this paper we report the strategies used for the preparation of the dendrimers, and their photophysical and electrochemical properties showing that incorporation of iridium(III) with one or three BTP ligands into a dendritic framework can give rise to solution processable phosphorescent red-light emitting films.

Results and discussion

Syntheses

The structures of and synthetic pathways to the two dendrimers are shown in Schemes 1 and 2. Both dendrimers contain 2-ethylhexyloxy surface groups and biphenyl based dendrons attached to the iridium(III) complex cores. These are the same dendrons and surface groups as used for the green-light emitting phosphorescent dendrimers^{7c} and illustrate one of the advantages of the dendrimer technology, that is, the modularity of dendrimer preparation. The cores of the two



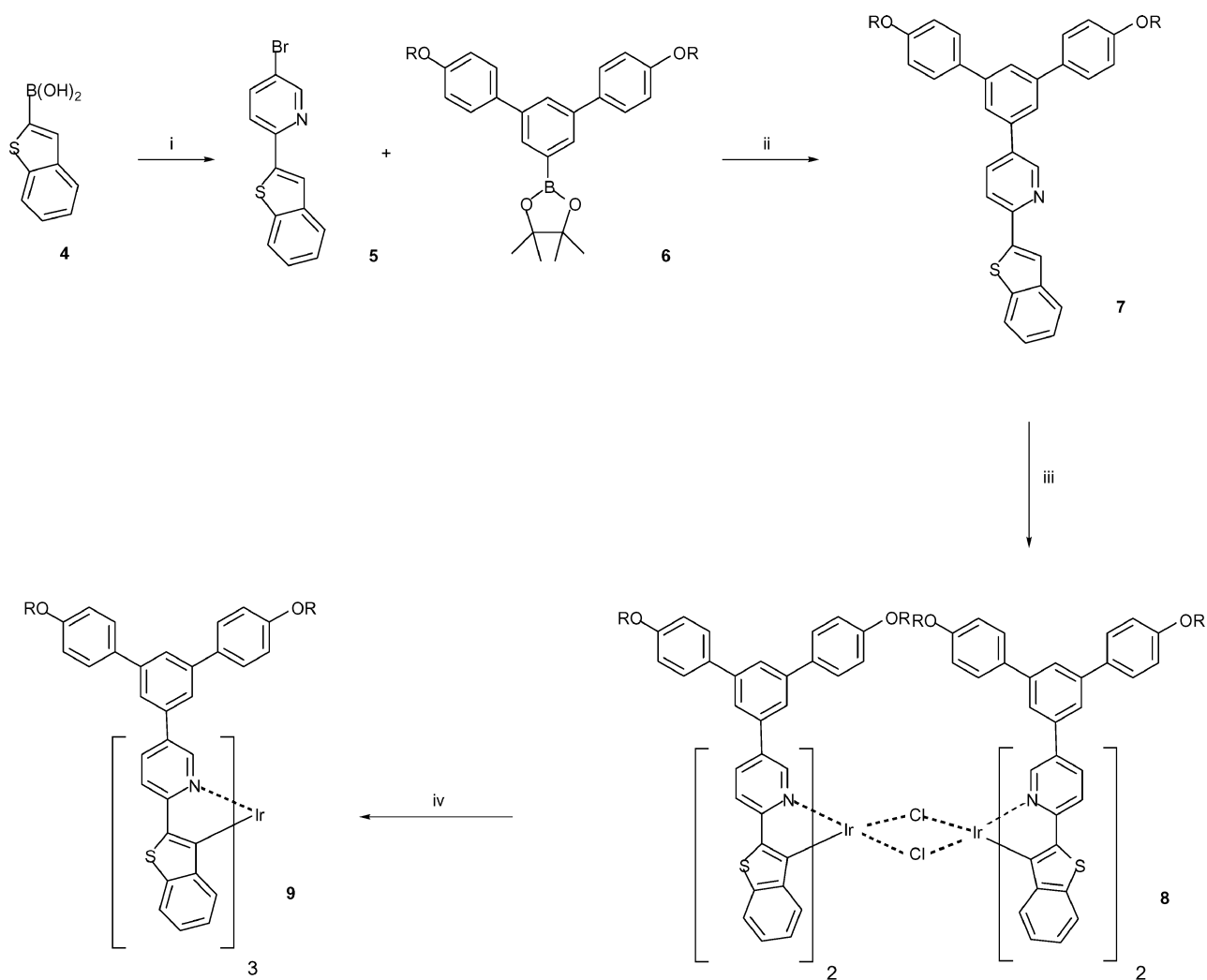
Scheme 1 Reagents and conditions: i, $\text{IrCl}_3 \cdot 3\text{H}_2\text{O}$, 2-EtOCH₂CH₂OH, H₂O, 130 °C; ii, 2-benzo[*b*]thiophene-2'-ylpyridine, $\text{AgOSO}_2\text{CF}_3$, 150 °C. R = 2-ethylhexyl.

dendrimers have important differences. The core of asymmetric dendrimer **3** (Scheme 1) is comprised of an iridium(III) cation complexed with two 2-phenylpyridyl ligands and one BTP ligand. Each of the 2-phenylpyridyl ligands has first generation dendrons attached *para* to the metal–carbon bond of the ligand phenyl and the dendrimer is denoted as G1-ppy₂BTPIr. The core of the symmetric dendrimer **9** (Scheme 2) has the iridium(III) complexed to three BTP ligands. Each of the BTP ligands has a first generation dendron attached to the pyridyl moiety and the complex is denoted as G1-BTP₃Ir.

Symmetric iridium(III) complexes are often prepared in a two step process from iridium(III) chloride trihydrate.^{11,12} The first step forms a chloro bridged iridium dimer which is then reacted in the melt with excess ligand to give the complex. The strategy for the preparation of asymmetric complex G1-ppy₂BTPIr **3** was to isolate the chloro bridged iridium dimer [G1-ppy₂IrCl]₂ **2** which was an intermediate in the formation of the symmetric green emitting dendrimer **10** (Fig. 1) and subsequently react it with the BTP ligand. [G1-ppy₂IrCl]₂ **2** was prepared by reaction of four equivalents of G1-ppy **1**¹² with iridium(III) chloride trihydrate in a 2-ethoxyethanol/water mixture heated at 130 °C. Crude [G1-ppy₂IrCl]₂ **2** precipitated from the reaction mixture and so was easily collected by filtration before further purification by chromatography. Under these conditions **2** was obtained in a yield of 77%. It is interesting to note that the MALDI–TOF spectrum of **2** only showed a very weak signal due to the dimer. However, two lower molecular weight isotopic clusters were easily observed. The higher molecular weight cluster of these two corresponded to half the dimer with the second lower molecular weight cluster corresponding to the

monomer less the chloride atom. It was important to remove G1-ppy **1** remaining from the preparation of **2** to avoid it acting in competition with the BTP ligand in the final complexation step. The complexation of **2** with BTP was sensitive to the reaction conditions. When the reaction was carried out in the melt at 150 °C for 16 hours with 50 equivalents of BTP in the presence of silver triflate the desired G1-ppy₂BTPIr **3** could be isolated in a 15% yield. The ¹H NMR spectrum of G1-ppy₂BTPIr **3** was much more complicated than that observed for the simple symmetric iridium(III) complexes. However, the integral ratios of the surface alkyl groups to the aromatic region of the spectrum corresponded to the stoichiometry of the complex. In addition, a MALDI–TOF mass spectrum had a cluster of peaks corresponding to the expected isotopic distribution of the molecular ion of G1-ppy₂BTPIr **3**. The stoichiometry was also confirmed by elemental analysis. The complexity of the ¹H NMR meant that it was not possible to determine whether a single isomer was formed. If fewer equivalents of BTP were used in the final complexation step then the yield of **3** was found to drop, primarily due to BTP subliming from the melt. If 50 equivalents of BTP ligand were used but the reaction time was increased to 67.5 hours then complexes were formed which could not be easily separated. MALDI–TOF mass spectral analysis of this mixture showed that in addition to the cluster of peaks associated with **3** there was a cluster of peaks around 1251.1 Daltons, which corresponds to the mass for the dendrimer with one G1-ppy ligand and two BTP ligands, **11** (Fig. 1).

The synthesis of the symmetric iridium complex, G1-BTP₃Ir **9**, is shown in Scheme 2. The first step in the synthesis was the



Scheme 2 Reagents and conditions: i, Pd(PPh₃)₄, Na₂CO₃, PhMe, EtOH, H₂O, 100 °C; ii, Pd(PPh₃)₄, Na₂CO₃, PhMe, EtOH, H₂O, Δ; iii, IrCl₃·3H₂O, 2-*n*-BuOCH₂CH₂OH, H₂O, 150 °C; iv, 7, AgOSO₂CF₃, 150 °C. R = 2-ethylhexyl.

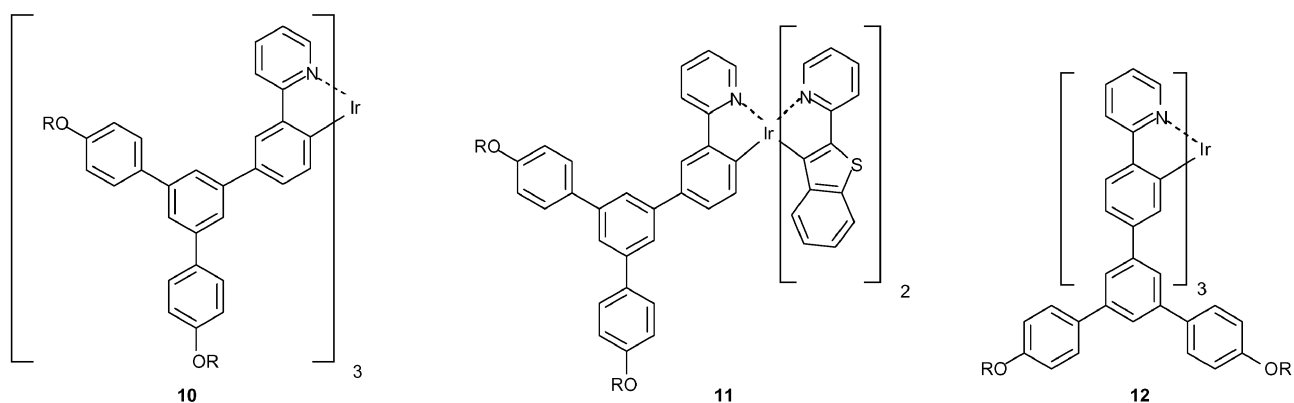


Fig. 1 Structures of 10, 11 and 12. R = 2-ethylhexyl.

coupling of commercially available benzo[*b*]thiophene-2-boronic acid **4** with one equivalent of 2,5-dibromopyridine using palladium catalysis. The Suzuki reaction was selective for the 2-position of the pyridine and Br-BTP **5** was isolated in a good yield of 82%. The synthesis of the “dendronised” BTP ligand, G1-BTP **7**, was completed by a final Suzuki cross-coupling of Br-BTP **5** with 1.3 equivalents of first generation boronate ester **6**.¹² Under these palladium catalysed conditions **7** was formed in a yield of 79%. The symmetric iridium dendrimer G1-BTP₃Ir **9** was formed by the normal two-step process. In the first step the chloro bridged iridium dimer [G1-BTP₂IrCl₂] **8** was formed

in 76% yield. As with **2** the MALDI-TOF spectrum of **8** showed two main isotopic clusters, one corresponding to half the chloro bridged dimer and the other, the same fragment but without the chlorine atom. **8** was then reacted at 150 °C for 17.5 hours with four equivalents of G1-BTP **7** in the presence of silver triflate to give G1-BTP₃Ir **9** in a yield of 20%. The simplicity of the ¹H NMR spectrum of G1-BTP₃Ir **9** indicated that the environment of each of the three G1-BTP ligands was identical, and was consistent with the formation of the *fac*-isomer.^{11b,c} The MALDI-TOF spectrum showed an isotopic cluster at the mass expected for the complex.

Both dendrimers, **3** and **9**, could be spin-coated to form good quality neat thin films or blend films with molecular materials such as 4,4'-bis(*N*-carbazolyl)biphenyl (CBP). Gel permeation chromatography (g.p.c.) showed that **3** and **9** were monodisperse. G.p.c. was also used to estimate the hydrodynamic radii of the dendrimers, which is used to correlate the effect of structure on the photophysical and electrochemical properties of the materials. The hydrodynamic radii (R_h) of the dendrimers were calculated using \bar{M}_v determined by g.p.c., and the Hester–Mitchell equation and Mark–Houwink relationship.¹³ The \bar{M}_v s of dendrimers **3** and **9** were 1360 and 1504 respectively and these correspond to hydrodynamic radii of 7.6 Å and 8.1 Å. The larger radius of **9** was expected as it has three dendrons whilst **3** has only two. However, the difference in hydrodynamic radii was not as marked as might have been expected based on the number of dendrons. The smaller than expected difference can be understood by considering the position of dendron attachment to the ligand. For example, with dendrimers comprising *fac*-tris(2-phenylpyridyl)iridium(III) cores and the same dendrons as used in this study there was a 25% difference in hydrodynamic radii depending on where the dendron was attached to the phenyl ring of the ligand.¹² When the dendron was *para* to the iridium–carbon bond as in **10** the dendrimer had a larger hydrodynamic radius than when the dendron was attached *meta* to the iridium–carbon bond as in **12** (Fig. 1). For **3** the two dendrons are *para* to the iridium–carbon bond whilst for **9** the three dendrons are *meta* to the ligand–metal bond although in this case it is an iridium–nitrogen dative bond. Therefore, in analogy to **10** and **11** with dendrons *para* and *meta* to the iridium–carbon bond respectively, each dendron of **3** should have a larger effect on the hydrodynamic radius than each of the dendrons on **9** and hence the difference in radii is not as large as might be expected. It is important to note that for **9** each of the emitting chromophores is protected by dendrons and hence should be less susceptible to intermolecular core–core interactions in the solid state.

Photophysical properties

The UV-visible absorption spectra of BTP, G1-BTP **7** and the two dendritic complexes are shown in Fig. 2. BTP has an onset to absorption at 348 nm with a π – π^* absorption maximum at 314 nm. The absorption spectrum of G1-BTP **7** has two absorption maxima. The long wavelength maximum at 334 nm arises from the dendron substituted BTP chromophore whereas the maximum at shorter wavelength (270 nm) is primarily due

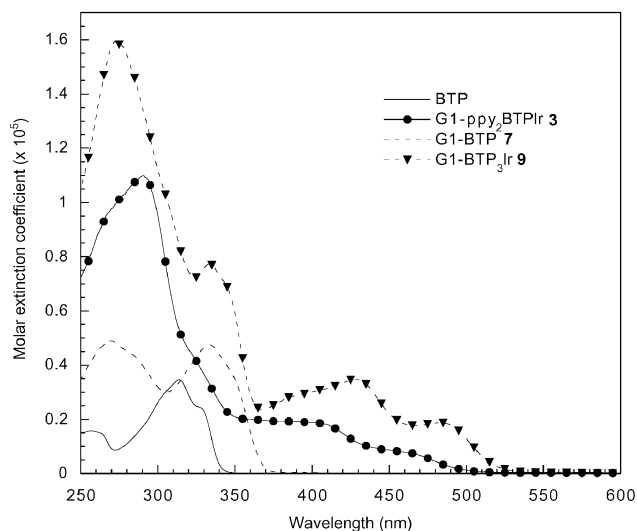


Fig. 2 Solution (dichloromethane) UV-visible absorption spectra of BTP, G1-BTP **7**, G1-ppy₂BTPIr **3** and G1-BTP₃Ir **9**.

to the biphenyl units in the dendrons. The red shift in the ligand absorption of G1-BTP **7** relative to BTP is due to the fact that the first phenyl ring of the dendron is in conjugation with the BTP moiety. For the symmetric iridium dendrimer **9** the complexation of the dendron to the metal cation makes little difference to the wavelengths of the ligand absorption. However, the molar absorption at around 270 nm increases in going from G1-BTP **7**, to asymmetric dendrimer **3** and symmetric dendrimer **9**. The increases in the molar absorption at this wavelength are due to an increase in the number of biphenyl units by two in the asymmetric dendrimer and three in symmetric dendrimer. For the asymmetric dendrimer **3** the absorption due to the BTP ligand at first sight appears to have moved significantly. However, the UV-visible absorption spectrum is complicated by the presence of the absorptions of the two G1-ppy ligands so that the BTP ligand absorption appears as a shoulder on the absorptions of the G1-ppy ligands. In addition to the ligand absorptions both **3** and **9** have two more absorption bands at wavelengths longer than 350 nm. These latter bands are the metal to ligand charge transfer (MLCT) transitions. The MLCT bands involve excitation of an electron from the HOMO that contains substantial metal orbital character to the ligand LUMO.^{11c,14} The MLCT bands are broad and are comprised of overlapping MLCT¹ and MLCT³ transitions¹⁴ and hence for **3** it is not possible to elucidate the absorptions of the MLCT states associated with each of the ligands. The red-shift in frequencies of the MLCT bands in going from G1-ppy₂BTPIr **3** to G1-BTP₃Ir **9** is consistent with the increased conjugation length of the ligand chromophore.

The photoluminescence (PL) spectra of **3**, **9** and **10** are shown in Fig. 3. In solution, **3** has two emission maxima at 599 nm and 650 nm and these two bands are shifted for **9** to 629 nm and 684 nm. These wavelengths are similar to those reported for simple molecular iridium(III) complexes containing two BTP ligands⁹ and correspond to emission of red light. For **3** there was no green emission from the MLCT states associated with the G1-ppy ligands although a contribution from the long wavelength side of their emission cannot be completely discounted (Fig. 3). However, if there was a significant contribution from the MLCT states associated with the G1-ppy ligands then the weighting of the emission peaks would be significantly different from the those reported for small molecules and this is not the case.⁹ Therefore, the emission

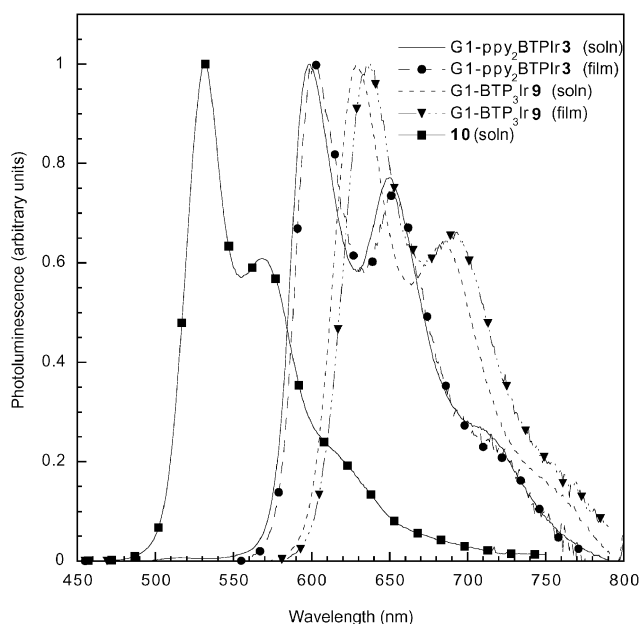


Fig. 3 Solution (soln) PL spectra of **3**, **9**, and **10** and film PL spectra of **3** and **9**.

from **3** occurs primarily or entirely from the localised MLCT states associated with the BTP ligand. The red shift in the PL spectrum of G1-BTP₃Ir **9** relative to **3** is consistent with the longer conjugation length of the ligand chromophore. For both **3** and **9** the film PL spectra were similar to the solution spectra but at slightly longer wavelengths (Fig. 3). This may be due to a different conformation, intermolecular interactions, or a different dielectric environment in the solid state. A final aspect of the PL study was to determine whether energy could be transferred efficiently from the dendrons to the core. For both dendrimers the photoluminescence excitation (PLE) spectra were collected with that of **3** being shown in Fig. 4 by way of example. For **3** the emission was observed at 600 nm and the excitation wavelength was scanned from 590 nm to 250 nm. The overlap of the PLE spectrum with the UV-visible absorption spectrum of **3** shows that not only does direct excitation of the core metal complex give rise to efficient core luminescence but even in the short wavelength region where the ligands and dendrons absorb there is excellent overlap. This shows that the energy absorbed by the biphenyl units in the dendrons is transferred efficiently to the core. The PLE spectrum of **9** also followed its UV-visible absorption spectrum closely across all wavelengths.

The photophysical properties of the dendrimers were probed further by measuring their photoluminescence quantum yields (PLQY) both in solution and the solid state. In solution the asymmetric dendrimer **3** had a PLQY of $47 \pm 5\%$ whilst the symmetric dendrimer **9** had a PLQY of $29 \pm 3\%$. The lower PLQY for the symmetric dendrimer **9** is consistent with the energy gap law where the longer wavelength emitters within a series of compounds tend to be less luminescent.¹⁵ In the solid state the PLQYs of **3** and **9** were found to drop significantly to $7 \pm 1\%$ and $10 \pm 1\%$ respectively. The drop in PLQY is indicative of luminescence quenching arising from increased interactions of the emissive cores. The decrease in PLQY in going from solution to the solid state is most dramatic for the asymmetric dendrimer **3**. For **3** the PLQY drops by a factor of 6.5 in going from solution to the solid state whereas for **9** the decrease is a factor of 2.7. The greater decrease in PLQY in going from solution to the solid state for **3** relative to **9** can be easily understood from their difference in structure. Asymmetric dendrimer **3** only has two dendrons and these are attached to the 2-phenylpyridyl ligands and not the BTP ligand, which in conjunction with the iridium(III) is responsible

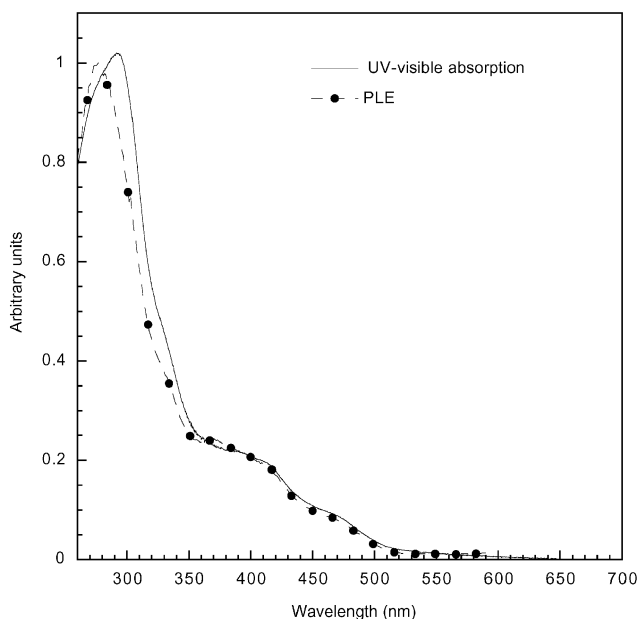


Fig. 4 Film UV-visible absorption and photoluminescence excitation (PLE) spectra of **3**.

for the MLCT emission. This means the emissive component of the core of the asymmetric dendrimer **3** is more open and susceptible to core-core interactions than the symmetric dendrimer **9**, which has dendrons on each of the BTP ligands. The quenching of the luminescence by intermolecular core-core interactions in the solid state was confirmed by measuring the PLQY of solid solutions of the dendrimers in CBP. Thin films of each dendrimer in CBP at a concentration of 20 wt% were prepared and the PLQYs of the **3**:CBP and **9**:CBP films were $49 \pm 5\%$ and $30 \pm 3\%$ respectively. These PLQYs are essentially the same as those measured for solutions of the two dendrimers and indicate that the dendrimers are evenly distributed in the CBP host, thereby avoiding the concentration quenching in the neat film.

To obtain a better picture of the excited state quenching processes in these materials, we have studied the photoluminescence decay transients using time-correlated single photon counting (TCSPC). We performed experiments in solution and CBP blends and compare the result with the neat films. All samples were excited at ~ 390 nm and the decays were detected at the peak emission wavelength. We have used a sum of two exponentials with lifetimes and pre-exponential factors of 2.2 μs (90%), and 0.3 μs (10%) respectively for the neat film of **3**, and 4.4 μs (90%), and 1 μs (10%) respectively for the neat film of **9**, in order to fit the observed decay. For each dendrimer in deoxygenated tetrahydrofuran solution and CBP blended film, the decays were single exponential and the lifetimes were almost the same, with **3** having a lifetime of 7.4 μs and **9**, 7.3 μs . These lifetimes are significantly longer than observed for neat films and consistent with the lower PLQY values of the neat films compared with solution and CBP blends. These lifetimes are also longer than those measured for the green emissive dendrimer **10**.¹² A longer triplet lifetime suggests that the spin-orbit coupling induced by the heavy metal atom is less significant.

Electrochemical properties

The electrochemical properties of the dendrimers were studied by cyclic voltammetry and the cyclic voltammograms are shown in Fig. 5. The $E_{1/2\text{S}}$ for the oxidations *versus* the

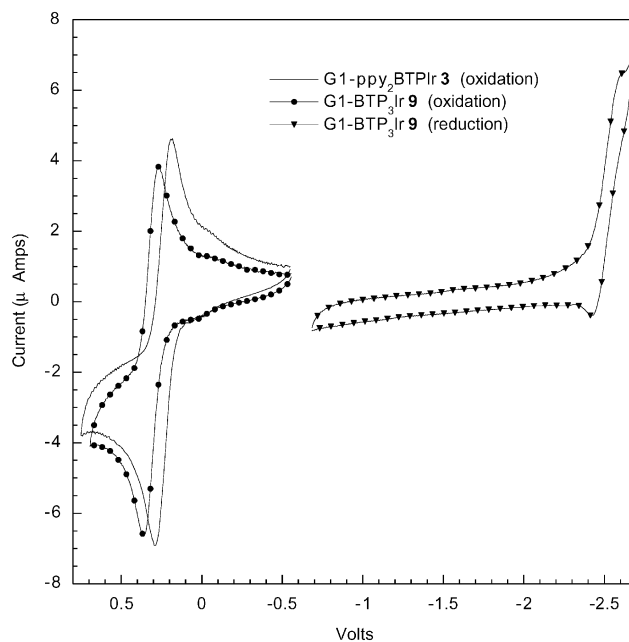


Fig. 5 Cyclic voltammograms *versus* the ferrocene/ferrocenium couple of G1-ppy₂BTPIr **3** and G1-BTP₃Ir **9**. Oxidation: Concentration = 1.0 mM, Scan rate = 100 mV s⁻¹, 0.1 M Bu₄NBF₄ in dichloromethane. Reduction: Concentration = 1.0 mM, Scan rate = 100 mV s⁻¹, 0.1 M Bu₄NBF₄ in THF.

ferrocene/ferrocenium couple were 0.24 V and 0.32 V for **3** and **9** respectively. The fact that the two potentials are similar can be understood by the fact that the HOMO of these complexes has substantial iridium character.^{11c,14} It is interesting to note that the oxidation potentials of **3** and **9** are similar to the green emitting phosphorescent dendrimers, for example **10**, that contain three of the same dendritic 2-phenylpyridyl ligands as in **3**. The oxidation potential of **10** has been reported to be 0.24 V.¹² Therefore, the difference in HOMO–LUMO energy gap between the two dendrimers must arise from a difference in energy of the LUMO. For these cyclometallated iridium complexes the LUMO is ligand based and so the reduction potential of **9** should be lower than that of **3**. We found that it was not possible to measure a chemically reversible reduction of either dendrimer in dichloromethane but found that a chemically reversible reduction could be observed for the symmetric dendrimer **9** in tetrahydrofuran. The $E_{1/2}$ for the reduction of **9** was -2.52 V. This reduction potential is more positive than the first reduction potential measured for the green emitting dendrimer **10**, which was at -2.91 V. These electrochemical results have important ramifications for device design as they indicate that there should be a similar barrier to injection of holes for the red and green materials but that electron injection should be easier for the red emitting materials. By using the oxidation potential and HOMO energy level for 4,4'-bis(*N*-3-methylphenyl-*N*-phenylamino)biphenyl (TPD) as a standard¹⁶ the HOMO of **3** was calculated to be 5.6 eV and the HOMO and LUMO for **9** were 5.7 eV and 2.9 eV respectively. For the asymmetric dendrimer **3** the first reduction was chemically irreversible even in tetrahydrofuran. However, the onset of the chemically irreversible reduction of **3** occurs at a more negative potential than that observed for **9** which is consistent with **9** having a lower LUMO energy than **3**.

In addition to using electrochemistry to determine the HOMO and LUMO energies it is interesting to note that the electrochemical band gap for **9** of 2.84 V corresponds to a wavelength of 437 nm. This wavelength is within the absorption band associated with the MLCT states suggesting that electrons and holes are injected into the orbitals associated with the MLCT states. That is, the electrochemical results show that charge is injected directly into the core chromophores of **3** and **9**, which is important for understanding charge transport in these materials.

Conclusion

We have demonstrated methodology for forming asymmetric and symmetric red emitting dendritic phosphorescent iridium complexes. The first generation dendrimers were solution processable and formed good quality neat and blended films. The asymmetric dendrimer illustrates that the emission of iridium(III) complexes can result from the MLCT states associated with the ligand with the lowest HOMO–LUMO energy gap and that the emission is not the average of all the ligands attached to the iridium. Comparison of the PLQYs of the symmetric and asymmetric dendrimers shows that having dendrons on the emitting chromophore decreases the core–core interactions and so reduces luminescence quenching in the solid state. Electrochemical analysis of the dendrimers showed that charge is injected directly into the cores.

Experimental

Measurements

NMR spectra were recorded on a Bruker DPX 400 MHz spectrometer: sp = surface phenyl; bp = branch phenyl; L = ligand. All J values are in Hertz. UV-visible spectra were recorded on a Perkin-Elmer UV-visible Lambda 14P spectrophotometer and were recorded as solutions in spectroscopic

grade dichloromethane. Mass spectra were recorded on a Micromass TofSpec 2E for matrix-assisted laser desorption/ionisation–time-of-flight (MALDI–TOF) from dithranol in reflectron mode, or a VG Platform for APCI. Melting points were recorded on a Gallenkamp melting point apparatus and are uncorrected. Microanalyses were carried out in the Inorganic Chemistry Laboratory, Oxford, UK. Gel permeation chromatography was carried out using PLgel Mixed-A columns (600 mm + 300 mm lengths, 7.5 mm diameter) from Polymer Laboratories calibrated with polystyrene narrow standards ($M_p = 580$ to 3.2×10^6) in tetrahydrofuran with toluene as flow marker. The tetrahydrofuran was degassed with helium and pumped with a rate of $1 \text{ cm}^3 \text{ min}^{-1}$ at 30.0°C . Light petroleum refers to the fraction of boiling point $40\text{--}60^\circ \text{C}$, unless otherwise stated. When solvent mixtures are used for chromatography over silica the proportions are given by volume.

Electrochemistry was performed on an EG&G Princeton Applied Research potentiostat/galvanostat model 263A with a glassy carbon working electrode, a platinum wire counter electrode and a Ag/3 M NaCl, sat. AgCl reference electrode. The supporting electrolyte was 0.1 M tetra *n*-butylammonium tetrafluoroborate, which was purified by recrystallisation from an ether–ethyl acetate mixture. Dichloromethane was purified by a literature method¹⁷ and distilled from calcium hydride before use. Tetrahydrofuran was distilled from sodium with benzophenone as a moisture indicator, then from lithium aluminium hydride before use. Potentials are quoted relative to the ferrocene/ferrocenium couple.¹⁸ Ferrocene was purified either by recrystallisation from ethanol or by sublimation.

Solution PLQYs were measured by a relative method using rhodamine 101 in ethanol¹⁹ at room temperature as a standard. The dendrimers were dissolved in tetrahydrofuran and freeze–thaw degassed. Photoluminescence spectra were recorded in a JY Horiba Fluoromax 2 fluorimeter.

Films for the solid state PLQYs were spin-coated from a chloroform solution with a dendrimer concentration of 10 mg ml^{-1} at 1000 rpm for 1 min to give a thickness of about 150 nm. Their PLQYs were measured using an integrating sphere in accordance with Greenham *et al.*²⁰ with a helium cadmium laser (Kimmon) as the excitation source. The excitation intensity was 0.2 mW at 325 nm and the sphere was purged with nitrogen during the measurements.

Excited state lifetime measurements were performed using time correlated single photon counting (TCSPC). Excitation was at ~ 390 nm from a pulsed laser diode (Picoquant) giving 10 pJ pulse^{-1} . The instrument response function was approximately 350 ps on the fastest scale. All measurements were performed at room temperature. The solution samples were measured in a 1 cm path length cuvette and were freeze–thaw degassed. Films were kept in a vacuum of $< 10^{-3}$ mbar during measurements. The decay kinetics were fitted by a sum of exponential functions: $I(t) = A_1 \exp(-t/\tau_1) + A_2 \exp(-t/\tau_2)$ with A and τ as the pre-exponential factor and excited state lifetime respectively. The quality of the fits was confirmed by random distribution of the residuals.

G1-ppy₂BTPIr **3**

A mixture of G1-ppy **1**¹² (1.62 g, 2.53 mmol), iridium(III) chloride trihydrate (223 mg, 0.634 mmol), 2-ethoxyethanol (20.2 cm^3) and water (6.7 cm^3) was heated under argon at 130°C for 15 h and then allowed to cool. The resultant solid was collected and purified by column chromatography over silica with dichloromethane–light petroleum (0:1 to 1:0) as eluent to give an orange-yellow solid of [G1-ppy₂IrCl]₂ **2** (412 mg, 77%). mp $276\text{--}277^\circ \text{C}$; (Found: C, 72.15; H, 6.85; N, 1.8. C₁₈₀H₂₀₈Ir₂Cl₂N₄O₈ requires C, 71.8; H, 7.0; N, 1.9%); $\lambda_{\text{max}}(\text{CH}_2\text{Cl}_2)/\text{nm}$ 276 ($\log(\epsilon/\text{dm}^3 \text{ mol}^{-1} \text{ cm}^{-1})$ 5.47), 322sh (4.88), 407 (3.84), 456 (3.73), and 492sh (3.04); δ_{H} (400 MHz;

CDCl₃) 0.90–1.01 (48 H, m, CH₃), 1.30–1.63 (64 H, m, CH₂), 1.72–1.84 (8 H, m, CH), 3.91 (16 H, m, OCH₂), 6.17 (4 H, d, *J* 8, L H), 6.91 (4 H, m, L H), 6.96–7.05 (20 H, m, sp H and L H), 7.53–7.69 (28 H, m, sp H, G1-bp H and L H), 7.78–7.89 (8 H, m, G1-bp H and L H), 8.06 (4 H, d, *J* 8, L H) and 9.41 (4 H, d, *J* 5, L H); *m/z* (MALDI) (Found: 1502.8 (34%), 1503.8 (38%), 1504.8 (100%), 1505.8 (88%), 1506.8 (68%), 1507.8 (42%), 1508.7 (25%) and 1509.8 (85%). C₉₀H₁₀₄IrClN₂O₄ requires 1502.7 (40%), 1503.7 (42%), 1504.7 (100%), 1505.7 (87%), 1506.7 (63%), 1507.7 (37%), 1508.7 (15%) and 1509.7 (5%). A mixture of **2** (90 mg, 0.030 mmol), BTP²¹ (0.317 g, 1.50 mmol) and silver trifluoromethanesulfonate (18 mg, 0.069 mmol) was heated under argon in the melt at 150 °C for 16 h. The residue was purified by column chromatography over silica with dichloromethane–light petroleum (2:3) as eluent to give an orange-yellow solid of **3** (15.4 mg, 15%), mp 166–167 °C; (Found: C, 73.6; H, 6.7; N, 2.5. C₁₀₃H₁₁₂IrN₃O₄S requires C, 73.6; H, 6.7; N, 2.5%; λ_{max}(CH₂Cl₂)/nm 276sh (log(ε/dm³mol⁻¹cm⁻¹) 5.01), 290 (5.04), 316sh (4.70), 412sh (4.26) and 464sh (3.91); δ_H(400 MHz, CDCl₃) 0.90–0.98 (24 H, m, CH₃), 1.30–1.60 (32 H, m, CH₂), 1.73–1.80 (4 H, m, CH), 3.90 (8 H, m, OCH₂), 6.76 (1 H, m, L H), 6.83–7.02 (13 H, m, sp H and L H), 7.10–7.19 (3 H, m, L H), 7.29 (1 H, dd, *J* 2 and *J* 8, L H), 7.44 (1 H, m, L H), 7.55–7.69 (16 H, m, sp H, G1-bp H and L H), 7.73 (2 H, d, *J* 1.5, G1-bp H) 7.74–7.79 (3 H, m, G1-bp H and L H) and 7.96–8.02 (4 H, m, L H); *m/z* (MALDI) (Found: 1678.5 (34%), 1679.4 (46%), 1680.5 (82%), 1681.4 (100%), 1682.4 (56%), 1683.4 (39%), and 1684.4 (13%). C₁₀₃H₁₁₂IrN₃O₄S requires 1678.8 (42%), 1679.8 (49%), 1680.8 (100%), 1681.8 (95%) 1682.8 (57%), 1683.8 (24%) and 1684.8 (9%).

Br-BTP 5

A suspension of benzo[*b*]thiophene-2-boronic acid (2.00 g, 11.2 mmol), 2,5-dibromopyridine (2.66 g, 11.2 mmol), tetrakis(triphenylphosphine)palladium(0) (519 mg, 0.449 mmol), aqueous sodium carbonate (2 M, 9 cm³), ethanol (9 cm³) and toluene (26.4 cm³) was deoxygenated by alternate exposure to vacuum and flushing with nitrogen several times. The reaction mixture was then heated to 100 °C for 20 h. After being allowed to cool dichloromethane (150 cm³) was added and the solution was washed with water (100 cm³), dried over anhydrous magnesium sulfate, filtered and then the solvent was removed. The residue was recrystallised from a dichloromethane–ethanol mixture to leave **5** (2.67 g, 82%), mp 162–163 °C, (Found: C, 53.8; H, 2.9; N, 4.6. C₁₃H₈BrNS requires C, 53.8; H, 2.8; N, 4.8%; λ_{max}(CH₂Cl₂)/nm 322 (log(ε/dm³mol⁻¹cm⁻¹) 4.53), and 334sh (4.42); δ_H(400 MHz, CDCl₃) 7.35–7.40 (2 H, m, L H), 7.68 (1 H, dd, *J* 0.5 and *J* 8, L H), 7.79–7.89 (4 H, m, L H) and 8.68 (1 H, dd, *J* 0.5 and *J* 2, L H); δ_C(100.6 MHz, CDCl₃) 119.3, 120.6, 121.7, 122.6, 124.2, 124.7, 125.3, 139.2, 140.3, 140.7, 143.5, 150.7 and 151.1; *m/z* (APCI⁺) 290.0 (MH⁺, 90%) and 291.9 (MH⁺, 100%).

G1-BTP 7

G1-B(OCMe₂)₂ **6**¹² (100 mg, 0.16 mmol), **5** (39 mg, 0.13 mmol), tetrakis(triphenylphosphine)palladium(0) (11 mg, 0.01 mmol), aqueous sodium carbonate (2 M, 0.1 cm³), ethanol (0.1 cm³) and toluene (0.3 cm³) was deoxygenated and then heated at reflux (with a bath temperature of 110 °C) under argon for 26 h. The mixture was allowed to cool to room temperature and diluted with water (5 cm³) and ether (7 cm³). The organic layer was separated and the aqueous layer was extracted with ether (3 × 5 cm³). The organic layer and the ether extracts were combined, washed with brine (10 cm³) and dried over anhydrous sodium sulfate. The solvents were completely removed and the residue was purified by column chromatography over silica using dichloromethane–light petroleum (0:1

to 1:4) as eluent followed by chromatotron over silica using dichloromethane–light petroleum (0:1 to 1:2.5) as eluent to give a colourless oil of **7** (92 mg, 99%). (Found: C, 80.8; H, 7.4; N, 1.9. C₄₇H₅₃NO₂ requires C, 81.1; H, 7.7; N, 2.0%); λ_{max}(CH₂Cl₂)/nm 270 (log(ε/dm³mol⁻¹cm⁻¹) 4.69), 283sh (4.65), 334 (4.68) and 345sh (4.60); δ_H(400 MHz, CDCl₃) 0.93–1.00 (12 H, m, CH₃), 1.34–1.62 (16 H, m, CH₂), 1.74–1.84 (2 H, m, CH), 3.93 (4 H, m, OCH₂), 7.04 and 7.63 (8 H, AA'BB', sp H), 7.38 (2 H, m, L H), 7.72 (2 H, d, *J* 1.5, G1-bp H), 7.78 (1 H, dd, *J* 1.5, G1-bp H), 7.84 (1 H, m, L H), 7.88–7.92 (3 H, m, L H), 8.03 (1 H, dd, *J* 8 and 2, L H) and 8.99 (1 H, dd, *J* 0.5 and 2, L H); δ_C(100.6 MHz, CDCl₃) 11.1, 14.1, 23.1, 23.9, 29.1, 30.5, 39.4, 70.6, 115.0, 119.5, 121.1, 122.6, 123.7, 124.1, 124.5, 125.1, 125.2, 128.3, 133.0, 135.1, 135.7, 138.4, 140.5, 140.7, 142.4, 144.6, 148.2, 151.5 and 159.4; *m/z* (APCI⁺) 696.3 (MH⁺, 100%).

G1-BTP₂Ir 9

A suspension of **7** (1.416 g, 2.034 mmol) and iridium(III) chloride trihydrate (311 mg, 0.885 mmol) in water (7.2 cm³) and 2-*n*-butoxyethanol (21.5 cm³) was deoxygenated then heated under argon at 130 °C for 17 h. After being allowed to cool the orange precipitate was collected by filtration and washed with methanol. The residue was purified by column chromatography over silica with dichloromethane–light petroleum (2:3) as eluent to give [G1-BTP₂IrCl]₂ **8** (1.08 g, 76%) as an orange solid. A sample for analysis was recrystallised from a dichloromethane–methanol mixture, mp 284–285 °C, (Found: C, 69.5; H, 6.5; N, 1.9. C₁₈₈H₂₀₈Cl₂Ir₂N₄O₈S₄ requires C, 69.8; H, 6.5; N, 1.7%; λ_{max}(CH₂Cl₂)/nm 2.74 (log(ε/dm³mol⁻¹cm⁻¹) 5.19), 315sh (4.89), 350sh (4.73), 368sh (4.67), 478sh (4.23) and 500 (4.39); δ_H(400 MHz, CDCl₃) 0.90–1.03 (48 H, m, CH₃), 1.30–1.64 (64 H, m, CH₂), 1.74–1.86 (8 H, m, CH), 3.84–3.98 (16 H, m, OCH₂), 5.61 (4 H, d, *J* 8, L H), 6.56 (4 H, m, L H), 6.93 (4 H, m, L H), 6.99–7.03 (20 H, m, sp H and L H), 7.33 (8 H, d, *J* 1, G1-bp H), 7.48–7.61 (24 H, m, sp H and L H), 7.86 (4 H, s, G1-bp H) and 9.97 (4 H, d, *J* 1.5, L H); *m/z* (MALDI) (Found: 1614.2 (39%), 1615.2 (44%), 1616.2 (100%), 1617.2 (84%), 1618.3 (72%), 1619.3 (53%), 1620.3 (29%) and 1621.3 (22%). C₉₄H₁₀₄ClIrN₂O₄S₂ requires 1614.7 (37%), 1615.7 (40%), 1616.7 (100%), 1617.7 (92%), 1618.7 (75%), 1619.7 (46%), 1620.7 (23%) and 1621.7 (9%). **8** (742 mg, 0.229 mmol), **7** (641 mg, 0.917 mmol) and silver trifluoromethanesulfonate (136 mg, 0.229 mmol) were dissolved in dichloromethane (3 cm³), stirred for a few minutes and then the solvent was removed. The flask was then heated under argon in an oil bath at 143 °C for 17.5 h and allowed to cool. The solid residue was purified by column chromatography over silica with dichloromethane–light petroleum (2:3) as eluent to give recovered **8** (169 mg, 23%) which co-chromatographed with and had an identical ¹H NMR spectrum to an authentic sample. A second fraction was collected and the solvent removed to leaving an orange solid which was recrystallised from a dichloromethane–methanol mixture to give **9** (208 mg, 20%) mp > 165 °C (decomp.), (Found: C, 74.3; H, 6.9; N, 1.9. C₁₄₁H₁₅₆IrN₃O₆S₃ requires C, 74.4; H, 6.9; N, 1.9%); λ_{max}(CH₂Cl₂)/nm 274 (log(ε/dm³mol⁻¹cm⁻¹) 5.20), 333 (4.87), 342sh (4.83), 393sh (4.44), 428 (4.52) and 484 (4.25); δ_H(400 MHz, CDCl₃) 0.86–0.92 (36 H, m, CH₃), 1.24–1.48 (48 H, m, CH₂), 1.59–1.67 (6 H, m, CH), 3.70 (12 H, m, OCH₂), 6.66 and 7.31 (24 H, AA'BB', sp H), 6.79 (3 H, m, L H), 6.88 (3 H, m, L H), 7.14 (3 H, m, L H), 7.33 (6 H, d, *J* 1.5, G1-bp H), 7.60 (6 H, m, L H and G1-bp H), 7.77 (3 H, m, L H), 7.83 (3 H, m, L H) and 7.88 (3 H, dd, *J* 8 and *J* 2, L H); *m/z* (MALDI) (Found: 2274.3 (23%), 2275.3 (46%), 2276.3 (81%), 2277.3 (100%), 2278.3 (81%), 2279.3 (52%), 2280.3 (25%) and 2281.3 (9%). C₁₄₁H₁₅₆IrN₃O₆S₃ requires 2274.1 (27%), 2275.1 (44%), 2276.1 (85%), 2277.1 (100%), 2278.1 (80%), 2279.1 (49%), 2280.1 (24%) and 2281.1 (10%). A third fraction contained excess **7**

(771 mg), which co-chromatographed with and had an identical ¹H NMR spectrum to an authentic sample.

Acknowledgements

We thank CDT Oxford Ltd for financial support. IDWS acknowledges support from a Royal Society University Research Fellowship.

References

- (a) M. A. Baldo, S. Lamansky, P. E. Burrows, S. R. Forrest and M. E. Thompson, *Appl. Phys. Lett.*, 1999, **75**, 4; (b) C. Adachi, M. A. Baldo, S. R. Forrest, S. Lamansky, M. E. Thompson and R. C. Kwong, *Appl. Phys. Lett.*, 2001, **78**, 1622; (c) C. Adachi, R. C. Kwong, P. Djurovich, V. Adamovich, M. A. Baldo, M. E. Thompson and S. R. Forrest, *Appl. Phys. Lett.*, 2001, **79**, 2082.
- J. C. Ostrowski, M. R. Robinson, A. J. Heeger and G. C. Bazan, *Chem. Commun.*, 2002, 784.
- (a) W. G. Zhu, C. Z. Li, L. J. Su, W. Yang, M. Yuan and Y. Cao, *J. Mater. Chem.*, 2003, **13**, 50; (b) Y. Y. Noh, C. L. Lee, J. J. Kim and K. Yase, *J. Chem. Phys.*, 2003, **118**, 2853; (c) M. J. Yang and T. Tsutsui, *Jpn. J. Appl. Phys.*, 2000, **39**, L828; (d) C. L. Lee, K. B. Lee and J. J. Kim, *Appl. Phys. Lett.*, 2000, **77**, 2280; (e) V. Cleave, G. Yahioglu, P. Le Barny, R. H. Friend and N. Tessler, *Adv. Mater.*, 1999, **11**, 285.
- (a) M. Venturi, S. Serroni, A. Juris, S. Campagna and V. Balzani, *Top. Curr. Chem.*, 1998, **197**, 193; (b) V. Balzani, P. Ceroni, A. Juris, M. Venturi, S. Campagna, F. Puntoriero and S. Serroni, *Coord. Chem. Rev.*, 2001, **219–221**, 545.
- M. Kawa and J. M. J. Fréchet, *Chem. Mater.*, 1998, **10**, 286.
- N. D. McClenaghan, R. Passalacqua, F. Loiseau, S. Campagna, B. Verheyde, A. Hameurlaine and W. Dehaen, *J. Am. Chem. Soc.*, 2003, **125**, 5356.
- (a) J. M. Lupton, I. D. W. Samuel, M. J. Frampton, R. Beavington and P. L. Burn, *Adv. Funct. Mater.*, 2001, **11**, 287; (b) S.-C. Lo, N. A. H. Male, J. P. J. Markham, S. W. Magennis, P. L. Burn, O. V. Salata and I. D. W. Samuel, *Adv. Mater.*, 2002, **14**, 975; (c) J. P. J. Markham, S.-C. Lo, S. W. Magennis, P. L. Burn and I. D. W. Samuel, *Appl. Phys. Lett.*, 2002, **80**, 2645; (d) T. D. Anthopoulos, J. P. J. Markham, E. B. Namdas, J. R. Lawrence, I. D. W. Samuel, S.-C. Lo and P. L. Burn, *Org. Elect.*, 2003, **4**, 71; (e) T. D. Anthopoulos, J. P. J. Markham, E. B. Namdas, I. D. W. Samuel, S.-C. Lo and P. L. Burn, *Appl. Phys. Lett.*, 2003, **82**, 4824.
- J.-P. Duan, P.-P. Sun and C.-H. Cheng, *Adv. Mater.*, 2003, **15**, 224.
- S. Lamansky, P. Djurovich, D. Murphy, F. Abdel-Razzaq, R. C. Kwong, I. Tsyba, M. Bortz, B. Mui, R. Bau and M. E. Thompson, *Inorg. Chem.*, 2001, **40**, 1704.
- V. V. Grushin, N. Herron, D. D. LeCloux, W. J. Marshall, V. A. Petrov and Y. Wang, *Chem. Commun.*, 2001, 1494.
- (a) S. Sprouse, K. A. King, P. J. Spellane and R. J. Watts, *J. Am. Chem. Soc.*, 1984, **106**, 6647; (b) H. G. Colombo, T. C. Brunold, T. Riedener and H. W. Güdel, *Inorg. Chem.*, 1994, **33**, 545; (c) A. B. Tamayo, B. D. Alleyne, P. I. Djurovich, S. Lamansky, I. Tsyba, N. N. Ho, R. Bau and M. E. Thompson, *J. Am. Chem. Soc.*, 2003, **125**, 7377.
- S.-C. Lo, E. B. Namdas, P. L. Burn and I. D. W. Samuel, *Macromolecules*, 2003, **36**, 9721.
- P. L. Burn, R. Beavington, M. J. Frampton, J. N. G. Pillow, M. Halim, J. M. Lupton and I. D. W. Samuel, *Mater. Sci. Eng. B*, 2001, **85**, 190.
- P. J. Hay, *J. Phys. Chem. A*, 2002, **106**, 1634.
- (a) J. V. Casper, E. M. Koeber, B. P. Sullivan and T. J. Meyer, *J. Am. Chem. Soc.*, 1982, **104**, 630; (b) J. V. Casper and T. J. Meyer, *J. Phys. Chem.*, 1983, **87**, 952.
- J. D. Anderson, E. M. McDonald, P. A. Lee, M. L. Anderson, E. L. Ritichie, H. K. Hall, T. Hopkins, E. A. Mash, J. Wang, A. Padias, S. Thayumanavan, S. Barlow, S. R. Marder, G. E. Jabbour, S. Shaheen, B. Kippelen, N. Peyghambarian, R. M. Wightman and N. R. Armstrong, *J. Am. Chem. Soc.*, 1998, **120**, 9646.
- D. D. Perrin and W. L. F. Amarego, *Purification of Laboratory Compounds*, Pergamon Press, Oxford, 1988.
- G. Gritzner and J. Kuta, *Electrochim. Acta*, 1984, **29**, 869.
- T. Karstens and K. Kob, *J. Phys. Chem.*, 1980, **84**, 1871.
- N. C. Greenham, I. D. W. Samuel, G. R. Hayes, R. T. Phillips, Y. A. R. R. Kessener, S. C. Moratti, A. B. Holmes and R. H. Friend, *Chem. Phys. Lett.*, 1995, **241**, 89.
- K. E. Chippendale, B. Iddon and H. Suschitzky, *J. Chem. Soc., Perkin Trans. 1*, 1972, **16**, 2023.